Forensic Science International 331 (2022) 111145

Contents lists available at ScienceDirect

Forensic Science International

journal homepage: www.elsevier.com/locate/forsciint

Forensic application of inverse and reverse projection photogrammetry to determine subject location and orientation when both camera and subject move relative to the scene[☆]

Geoffrey T. Desmoulin[a,*], Manraj Kalkat[a], Theodore E. Milner[a,b]

[a] GTD Scientific Inc., 2037 MacKay Avenue, North Vancouver V7P 2M8, Canada
[b] Department of Kinesiology and Physical Education, McGill University, Montreal, Canada

ARTICLE INFO

Article history:
Received 15 January 2021
Received in revised form 29 October 2021
Accepted 6 December 2021
Available online 18 December 2021

Keywords:
Inverse photogrammetry
Reverse projection
Bicycle accident

ABSTRACT

We present a case study of a mountain bicycle accident captured by the rider's chest-mounted action camera. The objective of the investigation was to determine the orientation of the bicycle relative to the ground and the location of the rider's center of gravity relative to the bicycle. The problem faced in the investigation was that the camera was moving relative to the scene and rider, and the bicycle was moving relative to the camera. Inverse photogrammetry was used to determine the location and orientation of the camera relative to the scene. Reverse projection photogrammetry applied to an exemplar bicycle provided an estimate of the location and orientation of the bicycle relative to the camera. The rider's position and orientation relative to the camera were estimated by comparing synchronized side views and chest-mounted action camera views of the rider's movements, recorded during a trail descent prior to the accident.

1. Introduction

Wearable action cameras have become popular for documenting sporting activities from a personal perspective as well as documenting events witnessed by first responders and law enforcement officers. The image quality of these devices has improved markedly over the past decade with advances in frame rate and image stability following suit. With the ability to obtain high resolution 3D laser scans of accident and crime scenes, there is the potential to use image sequences recorded by wearable action cameras to objectively reconstruct events based on principles of photogrammetry. The primary value of action camera documentation is that it provides a dynamic record of the sequence of events during an incident.

However, there are two important limitations that must be overcome in order to accurately represent the events. First, the action camera provides a limited perspective of the scene, i.e. from a vantage point on the wearer's body and this vantage point may be constantly changing in position and orientation as the wearer moves. Second, most action cameras produce images which are radially distorted due to the wide-angle nature of the lens. Methods have been devised for camera calibration, which can correct for radial distortion [1,8], and for determining the position and orientation of a camera in an external reference frame using control points in an image matched to locations in the reference frame [3]. Algorithms implementing these methods are now available in commercial software packages such as PhotoModeler. In forensic analysis, it may be necessary to determine the location and/or orientation of objects in the image relative to the camera where these objects were moving relative to both the camera and the external reference frame. This requires image processing techniques such as reverse projection photogrammetry [2,5].

We present a case study of a mountain bicycle accident where it was necessary to apply reverse projection photogrammetry to images recorded with a camera that was moving relative to the scene and relative to the bicycle. The case study illustrates how evidence from a wearable action camera can be used to reconstruct the events leading up to an accident and how the precision of the methodology can be determined.

1.1. Case presentation

This incident involves catastrophic failure of the steerer tube of a downhill mountain bicycle during impact of the front wheel with

☆ This research did not receive any specific grant from funding agencies in the public, commercial, or not-for-profit sectors.

* Corresponding author.
E-mail address: gtdesmoulin@gtdscientific.com (G.T. Desmoulin).

https://doi.org/10.1016/j.forsciint.2021.111145
0379-0738/

Fig. 1. Section of trail leading up to ramp jump (top) and section of trail below ramp (bottom).

the ground upon landing from a ramp jump. The steerer tube fractured close to the point where it inserted into the front fork, causing the fork to break away from the rest of the bicycle. The rider was thrown from the bicycle and suffered a spinal cord injury as the result of head first contact with the ground. The incident was recorded with an action camera (GoPro Hero HD) mounted on a chest harness worn by the rider.

At issue, was the orientation of the bicycle and the position of the rider's center of gravity relative to the point of contact of the front wheel with the ground. These two factors are critical in determining the ability of the rider to avoid being thrown from the bicycle after impact of the front wheel with the ground. The question was whether the rider could have avoided being pitched over the handlebar after impact if the steerer tube had not failed.

The incident setting was a downhill mountain bike trail where a sharp (approximately 90°) turn of the trail was followed by a ramp constructed from rough wooden planks built against a large tree and banked at approximately 45° (Fig. 1). Dimensions of the ramp were obtained from a land survey of the incident scene conducted several months later. The end of the ramp was approximately 1.4 m above the ground at its highest point. The trail dropped with a significant slope beyond the ramp and passed close to another large tree, located to the left of the trail, approximately 2 m from the edge of the ramp. The front wheel of the bicycle first touched the ground near the base of this tree. The survey data placed the point where the front wheel of the bicycle first touched the ground at approximately 2 m below the highest point on the ramp. A high-definition 3D laser scan of the incident scene was conducted 28 months after the incident as part of an investigation into the cause of the injury, providing data that could be used to determine the location and orientation of objects in a well-defined external reference frame.

2. Methodology

To determine the calibration parameters of the incident action camera, namely focal length, principal point and radial lens distortion, 29 2D calibration targets (April tags) were placed in various locations within an outdoor area at GTD Scientific Inc. headquarters, encompassing a similar 3D dimensional space to the area of interest at the incident site. Images of the calibration targets were then recorded with the incident camera from several different perspectives relative to the calibration space. A 3D scan of the calibration space was performed with a DOT3D scanner to create an accurate 3D point cloud locating the calibration targets in the calibration space. The centers of the calibration targets were then selected as control points for co-registration of the 2D camera images and 3D point cloud in PhotoModeler. The PhotoModeler software performed inverse photogrammetry to determine the camera calibration parameters.

The image corresponding to the first contact of the front wheel with the ground after the jump was identified from the incident video taken by the rider's action camera (Fig. 2). Five control points in the image were selected and matched to corresponding points in the 3D laser scan of the incident scene. PhotoModeler software then performed inverse photogrammetry to estimate the location and orientation of the camera in the reference frame of the 3D laser scan, hereafter referred to as the external reference frame. The PhotoModeler output provided the location of the center of the camera image in the coordinates of the external reference frame and the Cardan angles of the camera, which represent a sequential rotation around each coordinate axis required to bring the coordinate axes of the camera into alignment with the coordinate axes of the external reference frame. PhotoModeler represents the optical axis of the camera along the *z*-axis and the plane of the camera image as the *xy*-plane. The 3D laser scan represented gravitational vertical along the *y*-axis and the horizontal plane as the *xz*-plane, where the wooden ramp was traversed primarily along the negative *x*-direction (Fig. 2). The pitch angle, relative to the horizontal plane was of primary importance in this investigation. The pitch angle can be calculated using the rotation matrix specified by the Cardan angles by defining a vector along the optical axis of the camera and multiplying it by the rotation matrix. This transforms the vector so that it is represented in terms of the coordinates of the external reference frame. The pitch angle of the camera is equal to the cosine angle of the transformed vector relative to the horizontal plane.

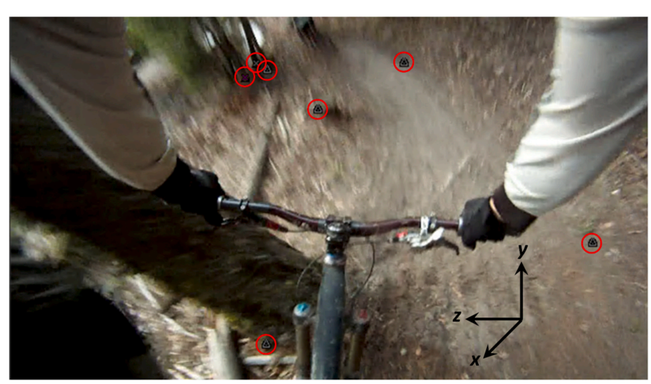

Fig. 2. Single frame from action camera image of bicycle and trail as front wheel touched the ground below the ramp. Control points are circled in red. Coordinate convention shown at bottom right. (For interpretation of the references to colour in this figure, the reader is referred to the web version of this article.)

PhotoModeler requires a minimum of 5 control points. To determine the precision of PhotoModeler's inverse photogrammetry algorithm when there are a limited number of control points available, 7 control points were selected from the action camera image (Fig. 2) and matched to positions in the point cloud of the 3D laser scan. The control points encompassed a large portion of the selected action camera image. The 7 control points served as a set from which the 21 possible subsets of 5 control points were created. These 21 subsets served as 21 different inputs to PhotoModeler. The 21 different outputs of PhotoModeler's inverse photogrammetry algorithm, i.e. the predicted locations and orientations of the camera, were then analyzed using descriptive statistics. The standard deviation provided an estimate of the precision of the inverse photogrammetry methodology.

The orientation of the bicycle frame and its position relative to the camera were estimated using reverse projection photogrammetry. The first step involved recording images of an exemplar bicycle, similar in all respects to the incident bicycle, with an action camera placed at various locations and orientations relative to the bicycle. The image recorded by the incident camera at the time that the front wheel contacted the ground served as the reference upon which the image of the exemplar bicycle was projected. The action camera location and orientation which produced the best superimposed match of the image of the exemplar bicycle to the reference image of the incident bicycle was taken to represent a valid estimate of the camera position and orientation relative to the bicycle at the time that the front wheel first contacted the ground during the incident.

Reverse projection photogrammetry is an empirical technique based on overlaying images recorded from different camera positions and orientations on a reference image. The objective is to find an overlay that produces the best match in order to identify the location and orientation of the camera which recorded the reference image. The action camera which had been worn by the rider in the incident was not available for this analysis. Therefore, a more recent model (GoPro Hero 8 Black) was used instead. Unlike the surrounding scene, the image of the bicycle in Fig. 2 is quite sharp because the rider is not moving relative to the bicycle. Therefore, we believe that the results of the reverse projection analysis should be representative of what would be obtained with an older model action camera. Magnified images of the fork crown of the exemplar bicycle, taken with the recent model camera, and the fork crown of the image shown in Fig. 2, which was taken with the incident camera, are compared in Fig. 3. Both images have the same pixel resolution, i.e. 1280 × 720. The comparison shows that the ability to detect a horizontal shift in fork crown position, illustrated by the parallel blue lines, is similar for the two cameras and is less than 1 mm. Short video segments of a stationary mountain bicycle were taken from different perspectives with the action camera. The height of the camera above the bicycle, the distance of the camera from the handlebar and the pitch angle of the camera were varied to obtain images from a variety of perspectives, corresponding to the range of locations over which an action camera, mounted on a rider's chest harness, would move. A sample image was then extracted from each video segment. Pairs of sample images from different camera positions were superimposed in Inkscape and carefully examined for matching of handlebar width and location of the damping control knobs on the front fork, as these are prominent features in the image which are sensitive to camera location and orientation (Fig. 4). The image from one camera position was used as a reference. The other image was made semi-transparent using Inkscape's Monochrome Transparency filter and its position was shifted until the handlebars of the two images were aligned. The superimposed images were then carefully examined for discrepancy in handlebar length and misalignment of the damping control knobs.

Fig. 3. Comparison of images of the fork crown of the exemplar bicycle (top), taken with a.
GoPro Hero 8, and the incident bicycle (bottom), taken with the incident GoPro, at the same scale. Parallel blue lines on the left of the images depict the minimum detectable horizontal shift in image position, which is similar for the two cameras and estimated to be 0.85 mm. (For interpretation of the references to colour in this figure, the reader is referred to the web version of this article.)

The location of the camera on the rider's body was estimated using a side view video of the rider during a jump from a small mound, which was recorded by a bystander earlier on the day of the incident. The video showed the rider moving through a range of postures from a near upright stance to a crouch with his hips well behind the bicycle seat. The orientation of the optical axis of the camera was estimated by comparing the images recorded with the action camera worn by the rider with corresponding the side view images. Features on the bicycle frame that appeared at the bottom of the field of view in an action camera image were mapped to the corresponding features in the side view image (Fig. 5). A line drawn from the center of the camera to a mapped feature, as it appeared in the side view image, represented the lower limit of the camera's vertical field of view. By measuring the angle between the line representing the lower limit of the camera's vertical field of view and a line joining the rider's left shoulder and hip. it was possible to estimate the amount by which the camera orientation changed as the rider changed his posture during the jump.

We selected a frame from the side view video when the rider was in a crouched position just prior to landing the jump. We marked the presumed location of the rider's joints in the video frame, measured their location relative to an arbitrary coordinate system and used anthropometry to estimate the location of his center of gravity in the image [7]. Since the location of the center of gravity of the exemplar bicycle was known, as well as the mass of the rider (85 kg) and the mass of the bicycle (17 kg), we were able to estimate the location of the combined centers of gravity of the bicycle and rider.

3. Results

The mean pitch angle of the camera was found to be −53.3° with respect to the horizontal at the time that the front wheel of the

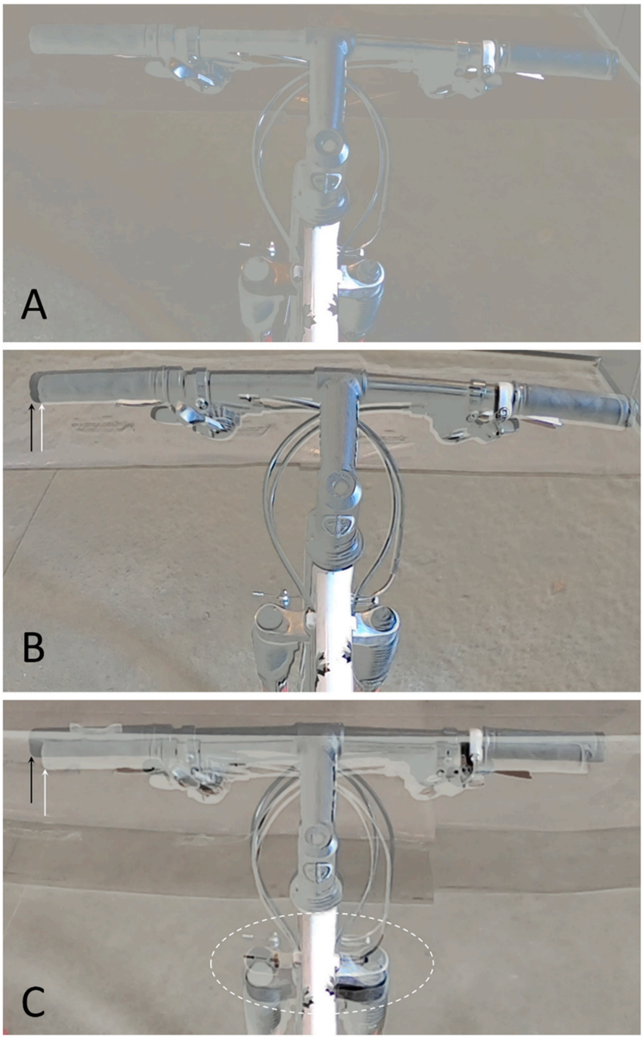

Fig. 4. Overlaid images of a mountain bike aligned on steerer tube clamp (center of images). A. Overlay of identical images serve as reference of perfect match. B. Overlay of images from same camera pitch angle but 1.5 cm difference in distance from the camera to handlebar stem. Dark and light arrows point to more and less distant camera positions, respectively. Note difference in handlebar alignment and length. C. Overlay of images from the same camera position, but with 1.5° difference in camera pitch angle. Dark and light arrows correspond to smaller and greater pitch angles, respectively. Note difference in handlebar alignment and length. Note difference in front fork alignment shown inside dashed oval.

bicycle first contacted the ground with a standard deviation of 1.8°. The precision in determining the location of the camera was estimated from the standard deviation in its Cartesian coordinates, which were 0.14 m along the *x*-axis (left/right from the rider's perspective), 0.10 m along the *y*-axis (gravitational vertical) and 0.19 m along the *z*-axis (principal direction of travel). Although this represents a significant degree of uncertainty in the location of the camera with respect to the trail, it does not have a direct bearing on the accuracy of the location and orientation of the camera relative to the bicycle.

The reverse projection photogrammetry indicated that the wheelbase of the bicycle was oriented approximately parallel to the optical axis of the camera, i.e. at −53.3° with respect to the horizontal plane (Fig. 6). From our analysis of reverse projected images of the stationary mountain bicycle, we found that differences in handlebar length and front fork alignment between the superimposed images could be reliably detected if the difference in camera pitch angle was 1.5° or greater. Similarly, differences in reverse projected images could be reliably detected if the difference in camera position was 1.5 cm or greater. Therefore, we consider the estimated distance from the camera to the handlebar stem to be accurate to within 1.5 cm and the pitch angle of the bicycle, i.e. the pitch angle of the wheelbase relative to the camera, to be accurate to within 1.5°. However, the uncertainty in the pitch angle of the bicycle relative to horizontal depends also on the uncertainty in the camera pitch angle. We assumed that the error in reverse projection photogrammetry was equivalent to the variance and used the method of combining variances to estimate the total uncertainty in the pitch angle, which gave an uncertainty of 2.3°, i.e. −53.3° ± 2.3°.

We found that the angle between lower limit of the camera's field of view and the line joining the shoulder and the hip generally varied between 65° and 75°, although it could drop as low as 60° or rise as high as 80°. As shown in Fig. 5, under the assumptions of our analysis, the combined center of gravity of the rider and bicycle was located 7.5 cm behind the point of contact of the front wheel with the ground along the horizontal direction. The point of contact of the front wheel with the ground in the figure is based on an assumed ground slope of 15°, based on consulting the topographical map of the trail, available on the trail website.

We examined the effect of uncertainty in the pitch angle on the location of the combined centers of gravity by rotating the bicycle to increase the pitch angle by 3° with respect to the horizontal. Note that this is greater than our estimated error in pitch angle of 2.3° but it serves to take into account the uncertainty of 1.5 cm in the distance from the handlebar stem to the camera. The 3° rotation moved the center of gravity forward by approximately 4.5 cm, which placed it approximately in line with the point of contact of the front wheel with the ground after taking into account the shift in contact location produced by rotation of the bicycle (Fig. 7). Assuming that the bicycle landed such that the center of gravity aligned with the point of contact of the front wheel, the motion of the rider's body would still depend on any evasive action that he took prior to and at the time of impact. The body position shown in Fig. 5 represents an

Fig. 5. Side view and chest mount view from video frames matched in time. Side view shows chest mount camera location. Dashed line from camera to front fork indicates lower limit of camera field of view. Angle between line from rider's shoulder to hip and lower limit of camera field of view indicated by dashed lines is equal to 75°.

Fig. 6. A. Estimated orientation of bicycle at instant of front wheel contact with the ground and location of combined rider/bicycle center of gravity (crossed circle), assuming ground slope of 15°. Dashed lines indicate optical axis and lower limit of camera field of view. B. Video frame illustrating rider position when landing from a jump. C. Image from B rotated to align with overlaid image of bicycle from A, illustrating postulated position of rider at instant that image in Fig. 2 was recorded.

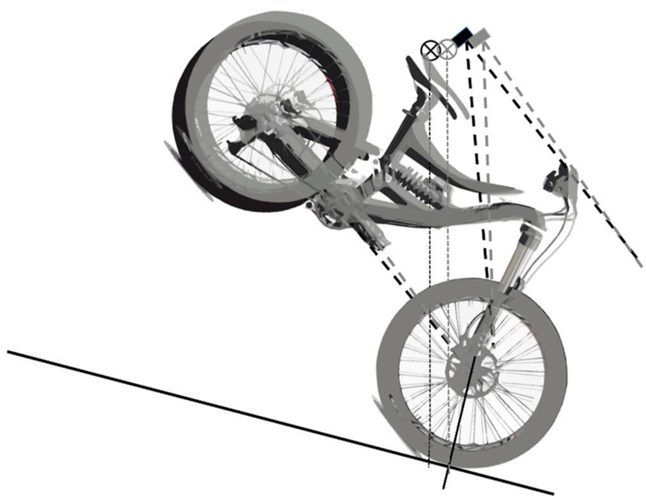

Fig. 7. Image of bicycle in Fig. 5A rotated counterclockwise by 3° to illustrate forward shift of center of gravity.

angle of 75° between the lower limit of the camera's field of view and the line joining the shoulder and hip. Our analysis of the side view video indicated that the rider was capable of crouching sufficiently to reduce this angle to 60°. Such action would keep the combined center of mass behind the point of front wheel contact with the ground.

4. Discussion

We have presented a case in which a combination of inverse photogrammetry and reverse projection photogrammetry was used to determine the orientation of a bicycle and rider at the time that the front wheel contacted the ground. Neither inverse photogrammetry nor reverse projection photogrammetry by itself would have been sufficient to establish whether or not there was potential for the rider to be pitched forward over the handlebar at the time of impact. However, by combining the two methodologies, the likely motion of the rider after impact could be established. Although reverse projection photogrammetry using CCTV video records has been previously used to determine the speed of an automobile [2,4–6], we are not aware of previous forensic applications of this methodology to action camera video images, nor for the purpose of determining the orientation of an object in space.

Our estimate of the most likely (mean) location of the combined centers of gravity of the bicycle and rider placed it 7.5 cm behind the point of contact of the front wheel when it first touched the ground after landing from the ramp. We determined that the uncertainty in our estimate of the location of the combined centers of gravity could have shifted it slightly ahead (1.5 cm) of the front wheel point of contact. However, this is very unlikely since it would have required the uncertainty to be almost maximal and exclusively in the direction of forward pitch. Considering that the uncertainty is equally likely to be in the direction of rearward pitch and that the probability of the uncertainty being maximal is very low, we can conclude that the location of the center of gravity of the bicycle/rider system was behind the front wheel point of contact with the ground. Thus, the torque created by gravity about the point of contact would most likely have resulted in the bicycle and rider pitching rearward toward the ground as the bicycle landed. Even in the unlikely event that the torque created by gravity created forward pitching, the torque would have been relatively small, given that our estimate that the maximum uncertainty would have placed the center of gravity only 1.5 cm ahead of the point of contact. The possibility existed for the rider to take evasive action by shifting his center of gravity farther to the rear of the bicycle, thereby moving the combined center of gravity farther away from the front wheel. A rearward shift of his center of gravity of more than 1.5 cm could have been achieved by shifting his hips rearward or removing his feet from the pedals and swinging his legs rearward.

The key outcome of this analysis is that there is a high probability that the rider would have avoided serious injury had the steerer tube not fractured upon impact of the front wheel with the ground. Because the front fork bent toward the bicycle frame when the steerer tube fractured, the point where the front wheel contacted the ground likely shifted behind the rider's center of gravity prior to separating completely from the bicycle frame. The unexpected shift in the contact point with the ground would have reduced the effectiveness of any evasive action taken by the rider. The subsequent separation of the front fork would have caused the front of the bicycle frame to drop launching the rider head first over the bicycle, an action compounded by the separation of the handlebar stem from the bicycle frame, leaving the rider without the ability to use his arms to slow his forward motion.

One of the limitations in our specific case is blurring of the scene due to motion of the camera relative to the scene. This reduces the ability to accurately match control points in the camera image and the 3D point cloud for inverse photogrammetry. Newer action camera models have features which significantly reduce blur due to camera motion, enabling control points to be identified with greater precision. The accuracy of reverse projection photogrammetry will be specific to the case under investigation since it depends on the distance and orientation of the objects of interest relative to the camera position. In our case, the image of the bicycle was sharp compared to the scene, allowing relatively accurate analysis with reverse projection photogrammetry. Obviously, having to work with a blurred image would reduce the ability to accurately determine the location and orientation of the camera. Therefore, it is important to bear in mind that the accuracy which we determined from our analysis is valid only for the case which we investigated. In general, the greater the distance from the camera to an object of interest, the lower the absolute accuracy since the camera can be moved over a greater distance before there is a detectable change in the location of the object in the camera image. On the other hand, the absolute accuracy of the orientation angles of the camera with respect to an object are affected both by the distance and the relative location of the object relative to the camera. More distant objects move more in the image than closer objects for a given change in camera angle. Objects which are aligned with the optical axis of the camera move relatively little in the image when the orientation of the camera changes compared to objects which are far removed from the optical axis, i.e. near the edges of the field of view. Therefore, the orientation angles of the camera can be determined with greater accuracy for objects which are near the edge of the field of view or which span a large proportion of the field of view, i.e. which extend to an edge of the field of view, than objects located in the center of the field of view and span only a small portion of the field of view.

This case study, which involves a single body mounted action camera, illustrates the potential of combining inverse photogrammetry and reverse projection photogrammetry of action camera images in forensic applications. The combination of techniques is particularly applicable to situations where both the object of interest and the camera are moving. Inverse photogrammetry places the camera in the scene whereas reverse projection photogrammetry places the object relative to the camera. For example, this methodology could be applied to video of a physical altercation if one of the subjects is wearing a body worn camera or to video taken by a dash mounted camera from a moving vehicle. In the case which we investigated, it was only by combining the two techniques that we were able to conclude that the forward pitching of the rider's body, which resulted in grave injury, was most likely caused by failure of the bicycle steerer tube.

CRediT authorship contribution statement

Geoffrey T. Desmoulin: Conceptualization, Project administration, Writing, Resources. **Manraj Milner:** Software, Investigation. **Theodore E. Kalkat:** Methodology, Writing, Visualization, Data curation and Validation.

Acknowledgements

The authors would like to thank the PhotoModeler Technologies for on-demand technical support during the investigation. Furthermore, the authors extend their gratitude to Ms. Christina Stevens (Operations Lead), for her continued support of R&D activities within our company, Mr. Tim Prokop (VP of Development) for turning topics such as this into visually interesting media that support our Science of Violence® course and overall marketing efforts, and for Mr. Petar Hristov who's technical assistance was invaluable in making this project a reality.

References

[1] C. Balletti, F. Guerra, V. Tsioukas, P. Vernier, Calibration of action cameras for photogrammetric purposes, Sensors 14 (2014) 17471–17490, https://doi.org/10.3390/s140917471
[2] B. Epstein, B.G. Westlake, Determination of vehicle speed from recorded video using reverse projection photogrammetry and file metadata, J. Forensic Sci. 64 (2019) 1523–1529, https://doi.org/10.1111/1556-4029.14053
[3] P. Grussenmeyer, O.A. Khalil, Solutions for exterior orientation in photogrammetry: a review, Photo Rec. 17 (2002) 615–634, https://doi.org/10.1111/0031-868X.00210
[4] W. Heng, H. Feng, C. Guan, S. Pan, W. Li, A vehicle motion reconstruction method based on vehicular video, Proc. ICMTMA (2020) 1003–1007.
[5] B. Hoogeboom, I. Alverink, Measurement uncertainty when estimating the velocity of an allegedly speeding vehicle from images, J. Forensic Sci. 55 (2010) 1347–1351, https://doi.org/10.1111/j.1556-4029.2010.01412.x
[6] A. Moser, H. Burg, Estimation of vehicle speed using video images and laser scanner data in PC-Crash, Proc. EVU (2017) 93–98.
[7] D. Winter, Biomechanics and Motor Control Of Human Movement, fourth ed., John Wiley and Sons, 2009, pp. 86–92.
[8] Z. Zhang, A flexible new technique for camera calibration, IEEE T Pattern Anal. 22 (2000) 1330–1334, https://doi.org/10.1109/34.888718